Intended for submission to *Chemistry of Materials*

Role of Binder in Sol-gel Synthesis of Ta_2O_5 Films for Photonic Crystal Fabrication

By

Nicholas Ndiege, Tabitha Wilhoite, Vaidyanathan Subramanian, Edmund G. Seebauer, Mark A. Shannon and Richard I. Masel*

***Corresponding author Professor Richard I. Masel**
Department of Chemical and Biomolecular Engineering
University of Illinois Urbana Champaign 600 S. Mathews, Urbana, IL-61801
Fax: (217) 333-5052
Email: r-masel@uiuc.edu

Corresponding author Prof. Richard Masel
Department of Chemical and Biomolecular Engineering
University of Illinois Urbana Champaign 600 S. Mathews, Urbana, IL-61801

Abstract

Advances in microelectromechanical systems has generated an ever growing demand for novel insulating material applicable to high temperature systems. Photonic bandgap materials are appealing for such applications, specifically Ta_2O_5 due to its high index of refraction, refractory nature and negligible absorbance in the infrared region. The challenge faced in the realization of such materials is the synthesis of Ta_2O_5 films whose thickness is in the order of a quarter wavelength of the incident infrared.

This work seeks to investigate the effect of addition of polyvinyl pyrollidone (PVP) binder material in the sol gel synthesis of thick, uniform and crack free Ta_2O_5 films. Incorporation of PVP into the sol precursor has enabled uniform and crack free films with thicknesses of up to 1.6 microns to be realized. Chemical probing of the precursor was conducted via TGA, FTIR, and NMR analysis of the sol to elucidate the processes behind this film formation. The calcined oxide films were characterized via SEM, XRD and XPS.

Keywords: Ta_2O_5 film, PVP, sol gel, thick films, photonic bandgap, photonic crystals

Introduction

Insulation for high temperature microelectromechanical systems has become a key area in research due to the development of microreactor systems that can attain wall temperatures in the order of 1200ºC.[1, 2] In order to add utility and portability to such systems it is required to thermally isolate parts of composite devices that incorporate such high temperature components. Thick refractory blocks (e.g. fibrous alumina) are the best mode of insulation currently available.

However, multilayer quarterwave photonic crystals have shown a tunabilty such as to exhibit a photonic bandgap in the infrared wavelength.[3] This is promising since at temperatures above 600ºC, IR radiation is the dominant mode of heat loss,[4, 5] thus a multitude of structures can be explored to insulate or anisotropically expel heat generated by microreactors.

The greatest challenge posed in realizing such materials is that photonic crystals with a bandgap in the IR calls for structures made out of dense refractory material with

thicknesses ranging from 1-5 µm.[3] Ta_2O_5 is the material of choice due to its high index of refraction, refractory nature and negligible absorbance in the infrared region.[4, 6, 7] Current deposition techniques typically attain thicknesses in the order of 1-1.5 µm.[7-14] Furthermore, these are achieved by use of high cost systems such as chemical vapour deposition, e-beam deposition etc. Any attempts at thicknesses beyond this range are hampered by slow growth rates and film cracking and delamination.[9, 15, 16] Solgel synthesis techniques are appealing due to their low cost and flexibility with regards to chemical tuning of the properties of the final material sought. Binder molecules such as ethylcellulose, polyethyleneimine (PEI), polyvinyl pyrollidone (PVP) and polyvinyl butyral (PVB) have been shown to increase film thickness with little or no cracking when incorporated in the sol precursor.[17-22] Previous studies have shown PVP to yield dense and thick Ta_2O_5 films on silicon with minimal or no cracking.[23] These films retained their stability even after prolonged heating at high temperature. Despite these discoveries, the mechanisms via which PVP facilitates the superior quality of oxide films still remains to be understood, hence in this paper, we seek to investigate the precise effect of the PVP binder molecule in the preparation of thick Ta_2O_5 films. The sol precursors were analyzed with time from the point of synthesis till 12 days later. Chemical probing was done via FTIR and NMR analysis. Thermogravimetric analysis (TGA) of the sol precursor was also performed. The resulting oxide films were characterized via scanning electron microscopy (SEM), X-Ray diffraction (XRD) and X-Ray Photoelectron Spectroscopy (XPS). The binder was found to have a viscosity increasing effect when incorporated into the sol precursor. This allowed for thicker films due to the increased surface tension during spin or dip coating. PVP also reduces the rate of solvent expulsion from the wet film and has been suggested to facilitate hydrogen bond formation within the film matrix, which limits crack formation during drying and high temperature sintering.[18, 24]

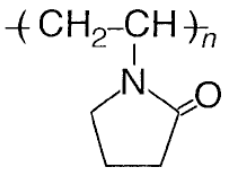

PVP

Experimental Section

Sol synthesis: 1-propanol (Aldrich® CAS# 71-23-8) was added to tantalum (V) ethoxide (Aldrich® CAS# 6074-84-6) in a 100ml round bottomed flask while stirring to prevent rapid hydrolysis of the latter when exposed to ambient moisture. PVP (Aldrich® CAS# 9003-39-8) (avg mw 1, 000, 000) was weighed out and 2-methoxyethanol (Aldrich® CAS# 109-86-4) added to it while stirring (molecular weight of PVP monomer was used in the calculations). The mixture was further sonicated for 15 minutes to achieve complete binder dissolution. The PVP & 2-methoxyethanol solution was then added to the tantalum(V)ethoxide & 1-propanol solution while stirring. The resulting mixture was then refluxed for 2 hours at 130ºC. This was followed by vacuum evaporation until a 12% loss in mass was attained. The solution was then let to cool to room temperature, after which acetylacetone (Aldrich® CAS# 123-54-6) was added yielding a deep yellow colored solution. The solution was let to stir for 20 hrs in a capped flask. This resulting sol was used for deposition by spin coating at various age points. Further details are discussed elsewhere.[23] The films were then left to dry in air for 24 hrs then subjected to a 9hr bake at 1000ºC under an O_2 flow of 100 cm^3/min. Temperature ramping rate was 1.6ºC/min for both up and down cycles. (fig. 1)

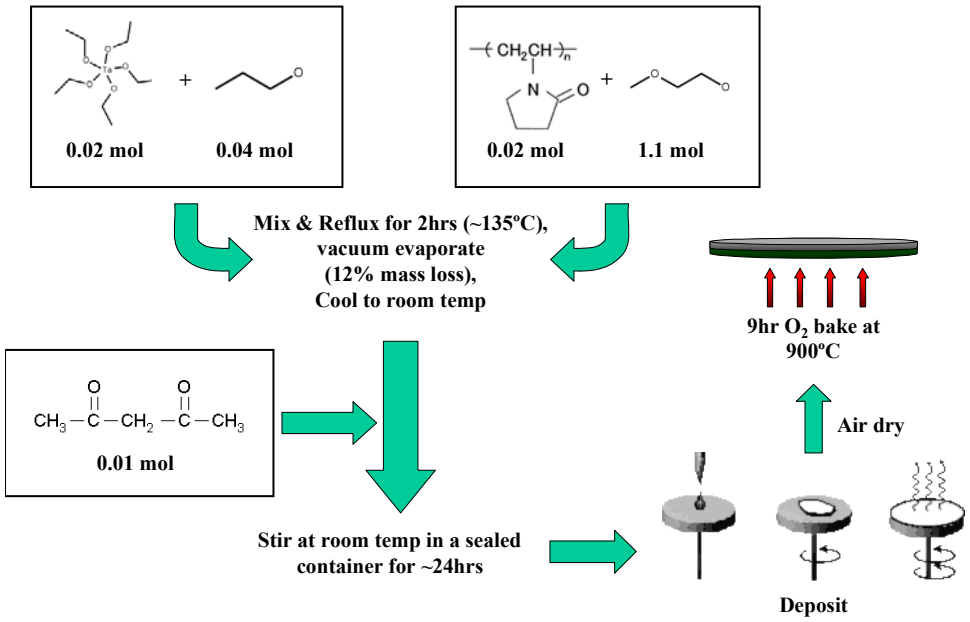

Figure 1: Sol gel scheme of synthesis & deposition of Ta_2O_5

Two control samples were synthesized; the first without PVP, and the second without acetylacetone.

Results

FTIR analysis: Given the strong positively charged Ta metal center bonded to negatively charged ligands, the large dipole moment typically yields characteristically strong IR bands for metallorganic compounds. Infra red analysis also reveals the presence of hydrogen bonds.[25, 26] Sampling for FTIR was in the form of dip coated liquid films on a silicon substrate, analyzed on a Magna IR Spectrometer 750® from Nicolet Instrument Corp. FTIR in the reflectance mode at 45º incidence angle. FTIR sampling of the sol and control sol (without acetylacetone) was conducted periodically starting at the end of sol synthesis, till the 12th day. (fig. 5 & 6). Spectra of the solvent (fig. 2) and PVP in 2-methoxyethanol solution (fig. 3) were also collected. Samples were Si <111> substrates (acetone-isopropanol rinsed) hand dipped in the respective sample at the indicated points in time.

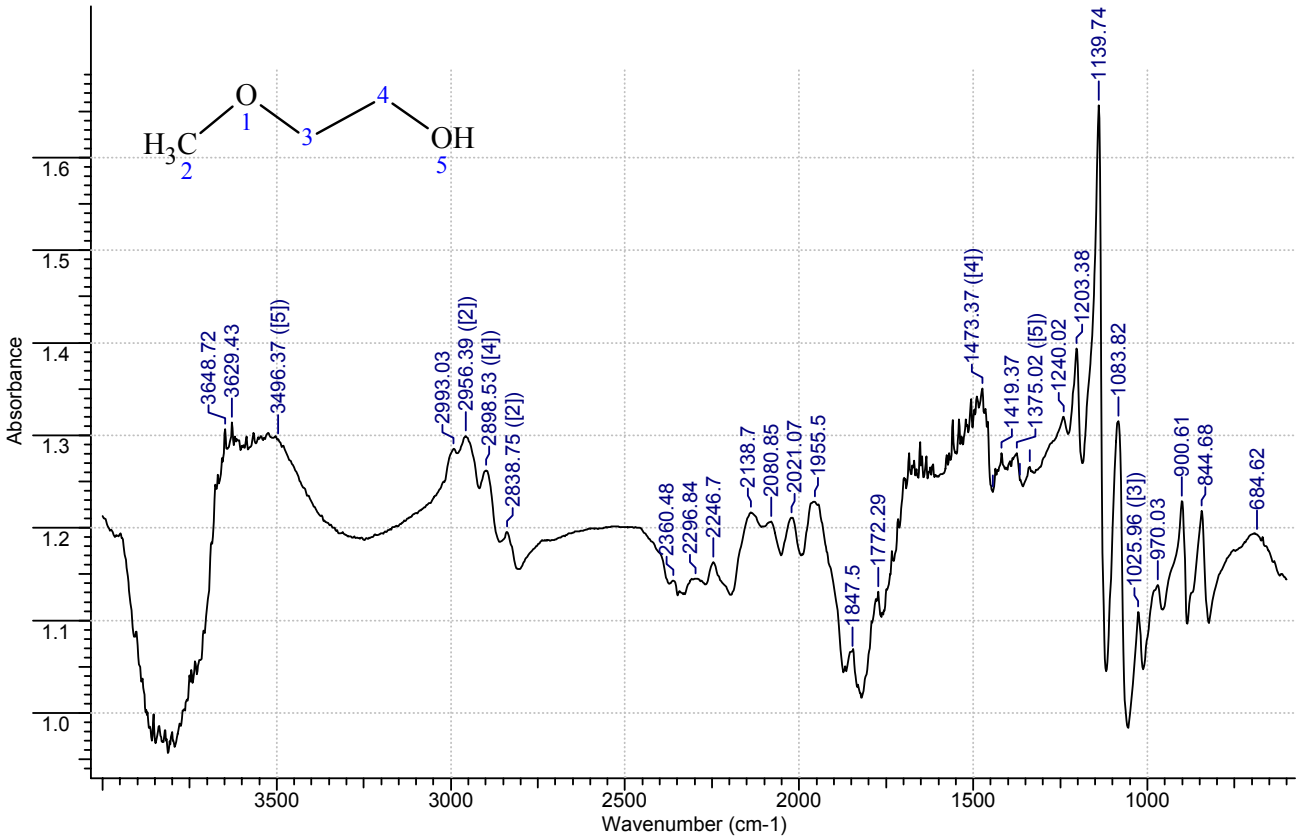

Figure 2: FTIR spectrum of 2-methoxyethanol film on Si<111>

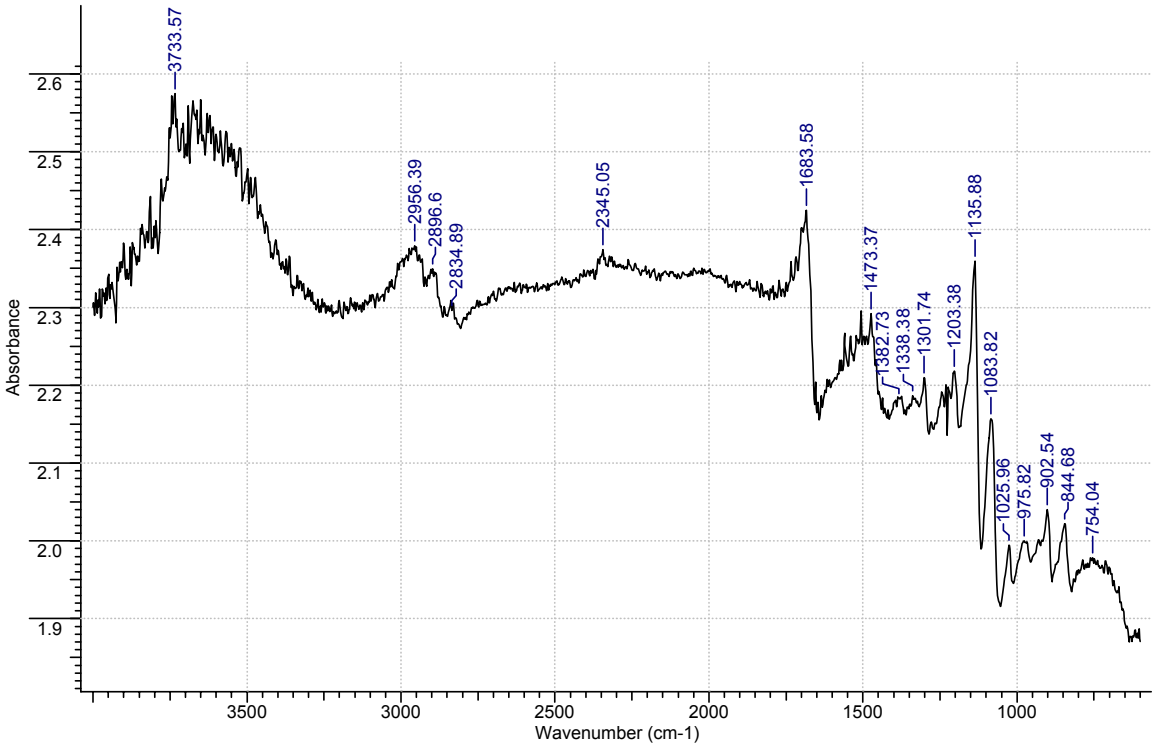

Figure 3 FTIR spectrum of PVP in 2-methoxyethanol film on Si<111>

cm^{-1}	Vibr/trans	ref
1025.96	CH_2 undefined	25, 26
1338.38	H-O in-plane bending	25-27
1375.02	H-O in-plane bending	25-27
1444.44	CH_3 umbrella mode	25, 26
1473.37	CH_2 scissoring	25, 26
2838.75	CH_2 sym stretching	25, 26
2898.53	CH_2 sym stretching	25, 26
2956.39	CH_3 asym stretching	25, 26
3496.37	O-H stretching	22, 25-28
1139.74	Si-O stretch	25, 26
1083	Si-O stretch	8, 25, 26
2080-2250	Si-H stretching	25, 26
1640-1690	C=O stretching	22, 25, 26, 28
1297	C-N stretch	22, 25, 26, 28
1383	C-H bending	22, 26, 28
1099-1053	Ta-O-C	8, 27, 29
<1000	(Ta-O) stretch, bend and torsion modes	8, 27, 29

Figure 4: FTIR table of assigments

Analysis of sol with acetylacetone:

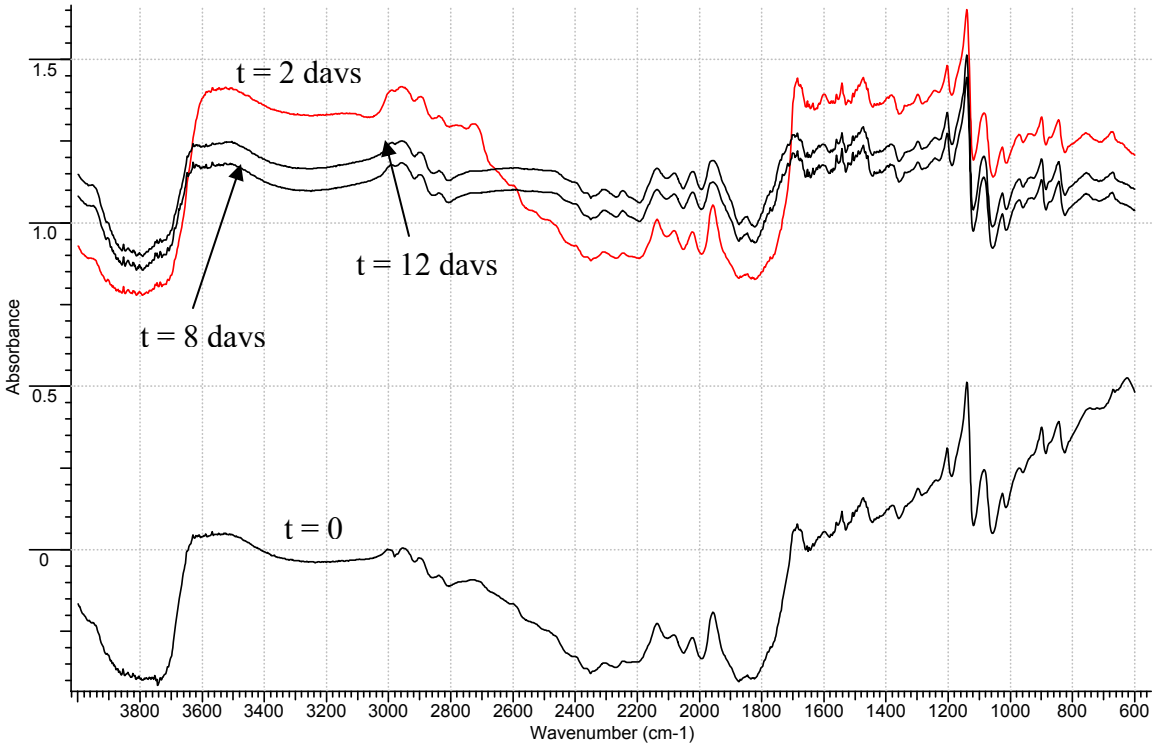

Figure 5: FTIR spectra of sol containing acetylacetone

Spectrum is identical to that of 2-methoxyethanol (fig. 2) except for C=O stretch at 1700cm^{-1}, 1297cm^{-1} C-N stretch and two bands at 650 cm^{-1} and 770 cm^{-1} attributable to Ta-O or Ta-O-C modes[27, 29]. The spectra obtained do not show any noticeable change with time. ^{13}C and ^{1}H NMR spectra show no change with time either.

Analysis of sol without acetylacetone:

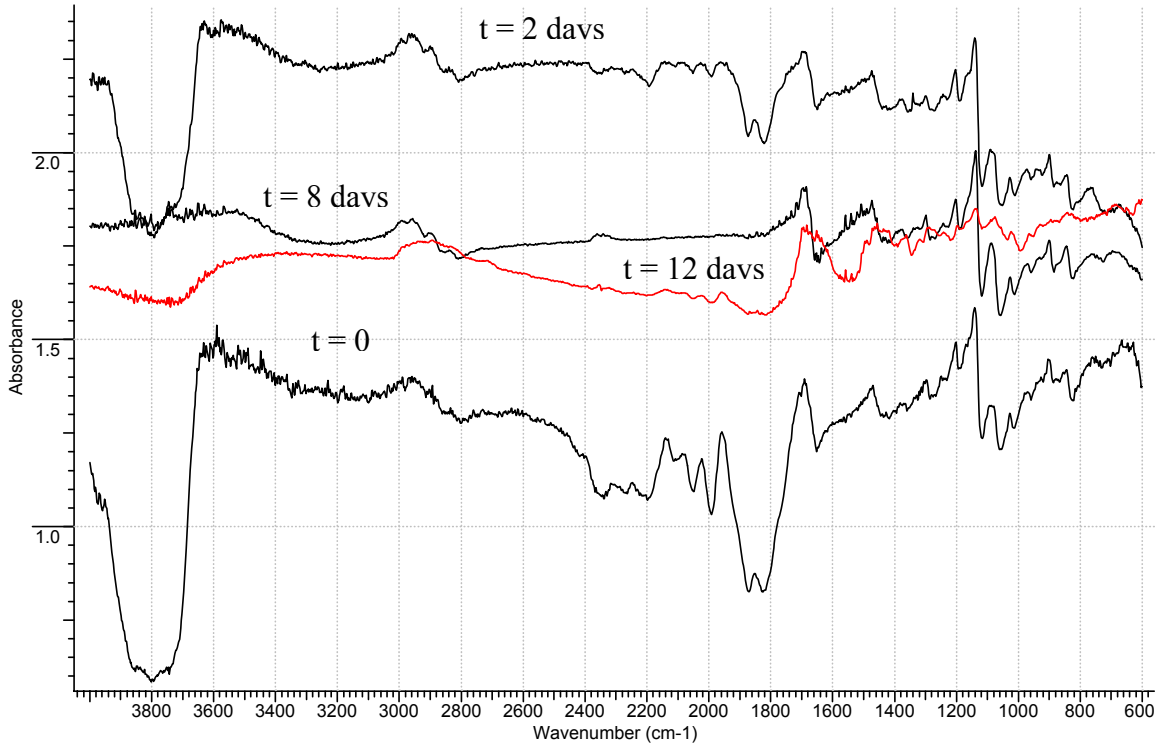

Figure 6: FTIR spectra of control sol (no acetylacetone)

Initially identical to 2-methoxyethanol (fig. 2) except for 1297cm^{-1} C-N and 1690cm^{-1} C=O stretch modes. With time, OH and methoxy CH_2 & CH_3 bands broaden out, leaving only the 1297cm^{-1} C-N, 1472 cm^{-1} CH_2 scissoring, 1690cm^{-1} C=O and 1140 cm^{-1} Si-O bands distinctly visible.[25, 26] Two bands at 650 cm^{-1} and 770 cm^{-1} attributable to Ta-O or Ta-O-C modes are present but broad and not as distinct as observed for the sol precursor.[27, 29] The broad OH band at ~3600 diminishes in relative intensity with time. The sol visibly turns turbid with time. ^{13}C and ^{1}H NMR spectra taken over time do not show any change. The sample had solidified after the 12th day.

NMR analysis: ^{1}H and ^{13}C NMR analysis was performed using Varian UNITY 400® and Varian UNITY 500® systems using Wilmad 528-PP-7® sample tubes. This analysis was important in determining what ligands are attached to the metal center at the end of the synthesis, as well as the fate of the exchanged hydrocarbon groups.[30, 31] NMR sampling was conducted daily over a period of 3 days starting at the end of sol synthesis, and thereafter every 2 days till the 18th day from the end of synthesis. The NMR standard used was duterated chloroform 99.8 atom % D with 1 % (v/v) TMS. The different samples analyzed were:

- Sol synthesized above (fig. 1)
- Sol synthesized as above but without PVP
- All the above but with $CaSO_{4(s)}$ pellet acting as H_2O scavenger
- Sol synthesized as above but without acetylacetone

There was no variation in the ^{1}H and ^{13}C spectra obtained from the ageing samples, except for a random shift in the upfield broad band appearing in all the ^{1}H spectra of ± 0.5 ppm (fig. 7 & 8). Spectra obtained from the control samples were similar to the spectra of the actual precursor.

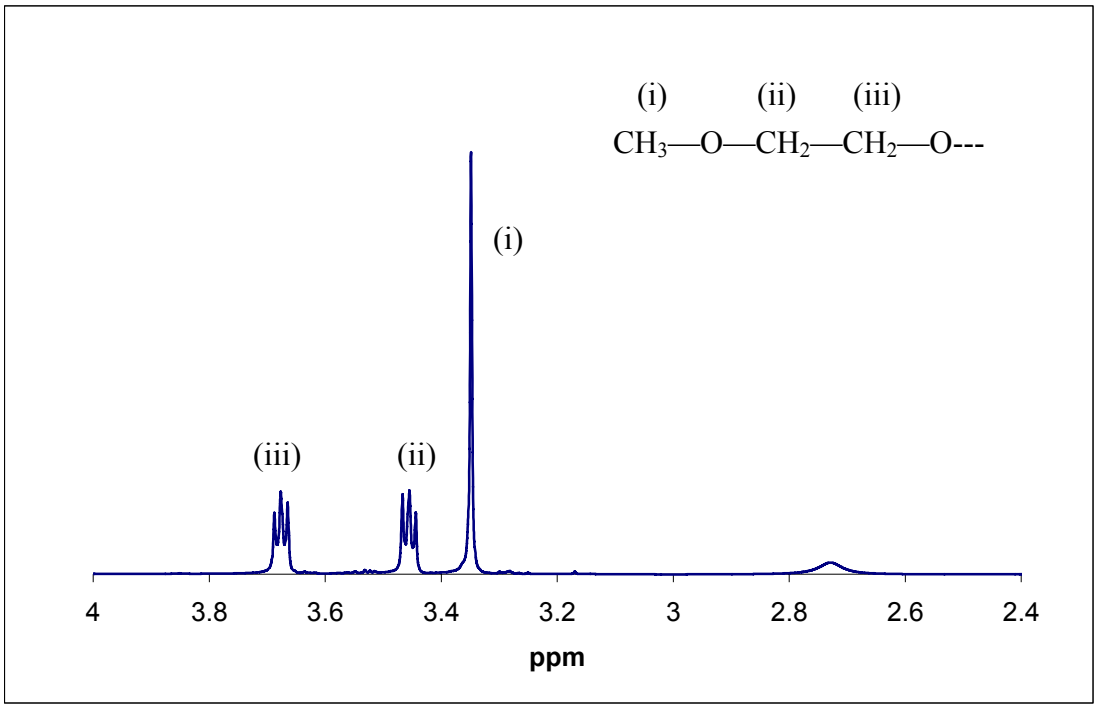

Figure 7: ^{1}H NMR of Ta_2O_5 precursor (freshly synthesized sol)

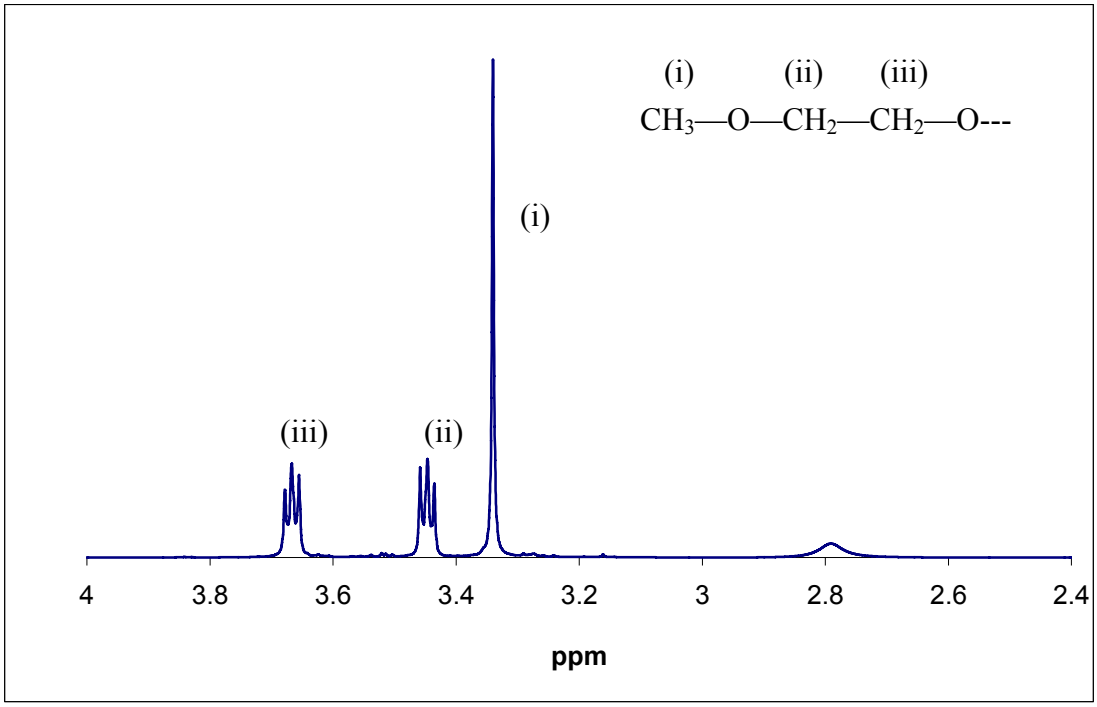

Figure 8: ^{1}H NMR of Ta_2O_5 precursor (sol is 3 days old)

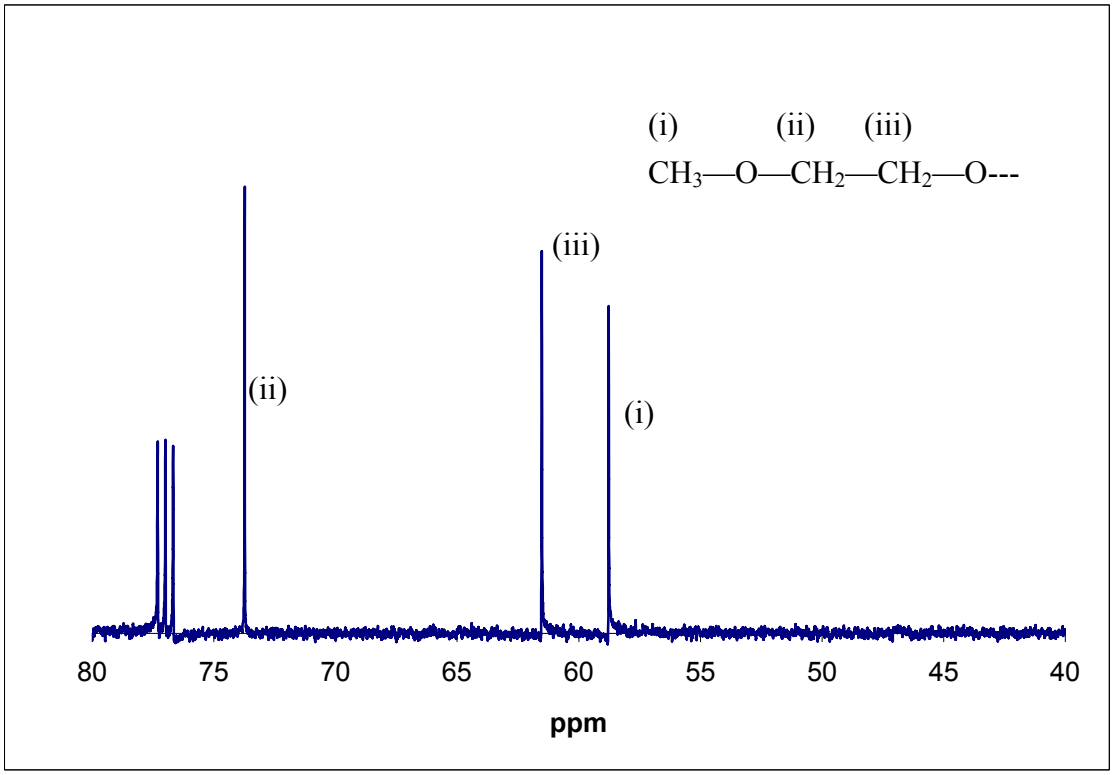

Figure 9: ^{13}C NMR of Ta_2O_5 precursor

SEM analysis: Scanning Electron Microscopy (SEM) was performed on samples of green (uncalcined) films and resulting oxide films to examine the microstructure resulting from the sols of different ages. Analysis was done on JEOL 6060LV® SEM machine. (fig 10 & 11)

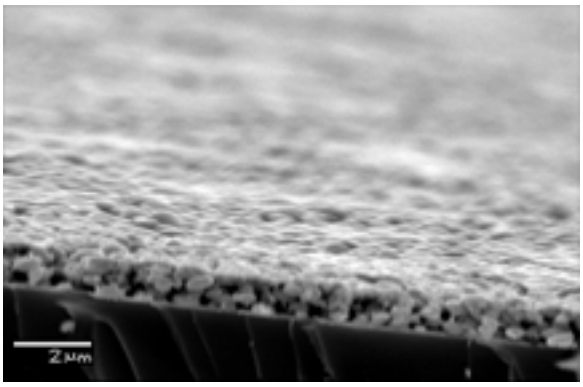

(a) Ta_2O_5 film deposited on Si at t = 0 hrs

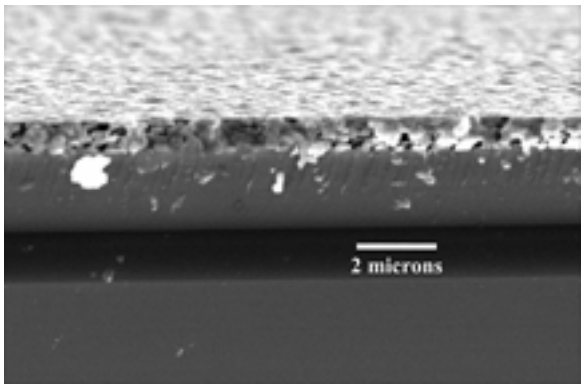

(b) Ta_2O_5 film deposited on Si at t = 12 hrs

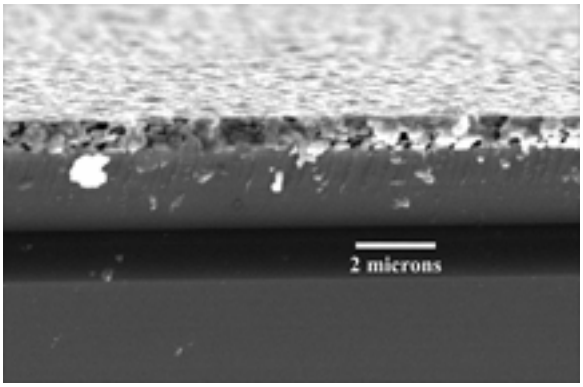

(c) Ta_2O_5 film deposited on Si at t = 24 hrs

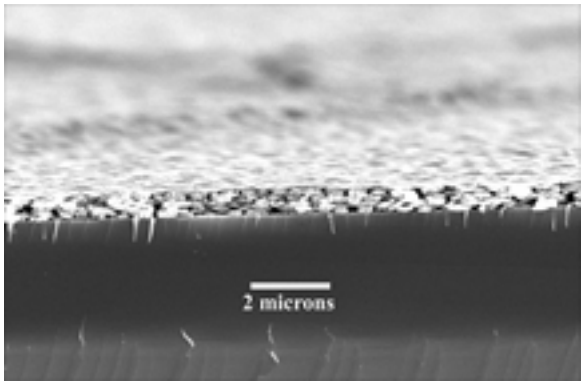

(d) Ta_2O_5 film deposited on Si at t = 48 hrs

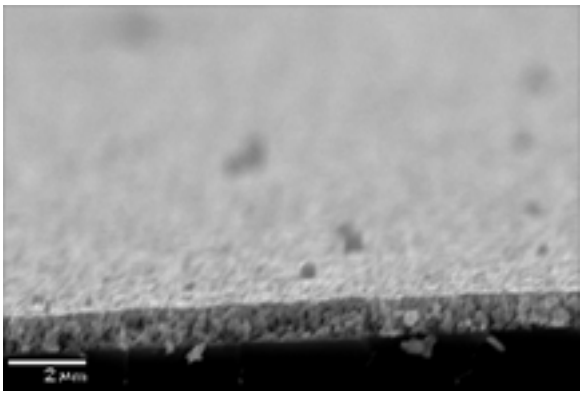

(e) Ta_2O_5 film deposited on Si at t = 8 days

Figure 10: SEM micrographs of calcined Ta_2O_5 films on Si <100> deposited from sols of varying age

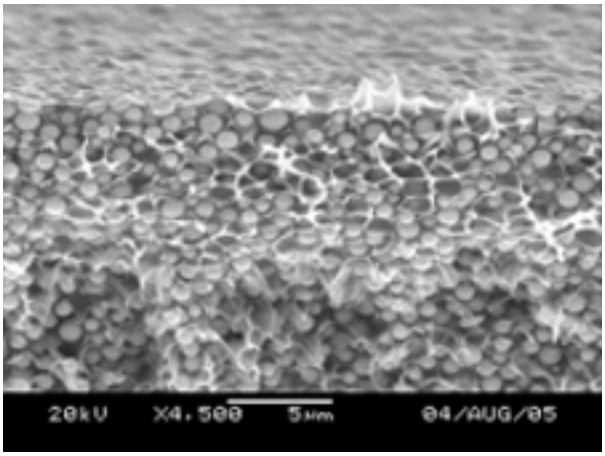

(a) green film from fresh sol with acetylacetone

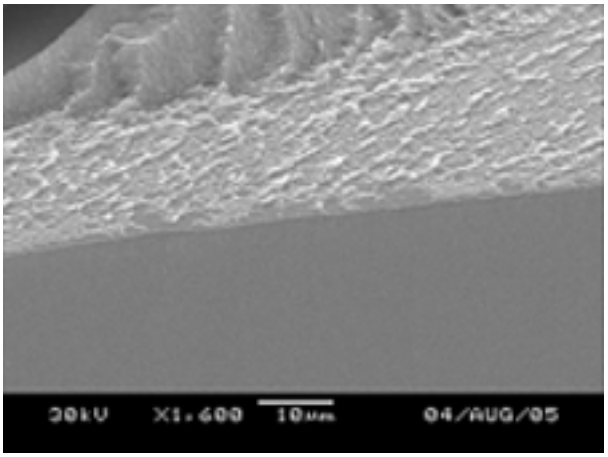

(d) green film from fresh sol without acetylacetone

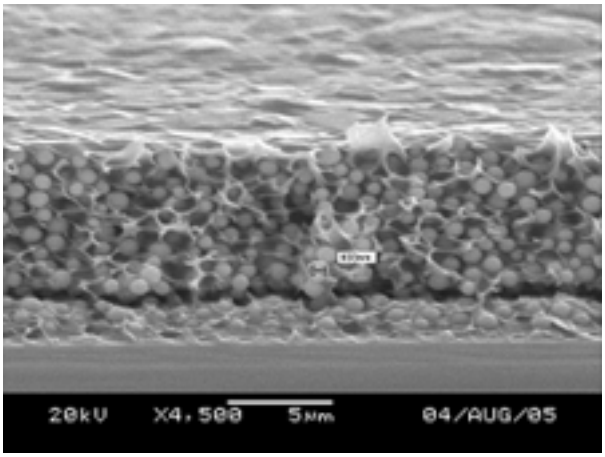

(b) green film from 5 day old sol with acetylacetone

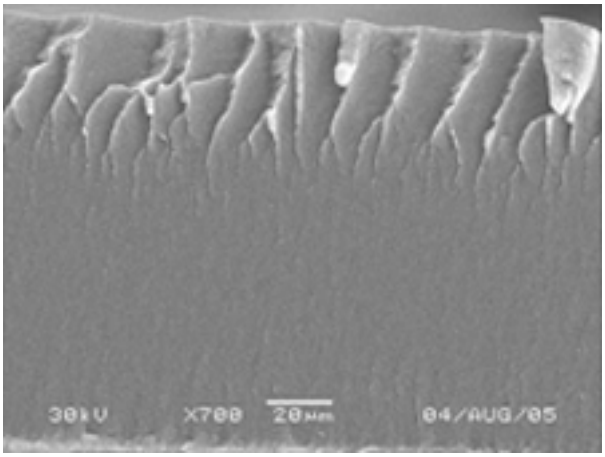

(e) green film from 5 day old sol without acetylacetone

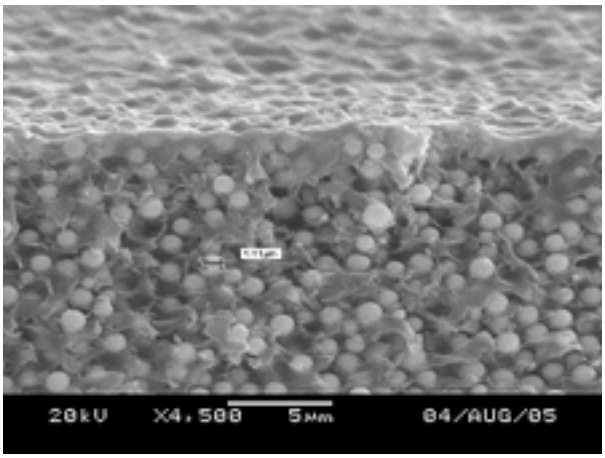

(c) green film from 12 day old sol with acetylacetone

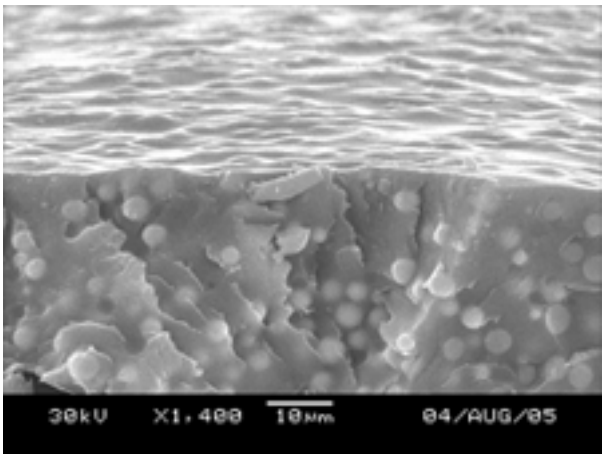

(f) green film from 12 day old sol without acetylacetone

Figure 11: SEM micrographs of green Ta_2O_5 films on Si <111> deposited from sols of varying age [(a),(b),(c): sol with acetylacetone; (d),(e),(f): sol without acetylacetone]

XPS analysis: X-ray photoelectron spectroscopy was used to analyze the residual carbon content of the Ta_2O_5 films after calcination on a PHI 5400® XPS system (Mg Kα x-ray source). Analysis was done on the oxide upper surface and within the film (surface was sputtered with Argon for 15 minutes). XPS was also used to reveal the Ta:O:C atomic ratio. (fig. 12)

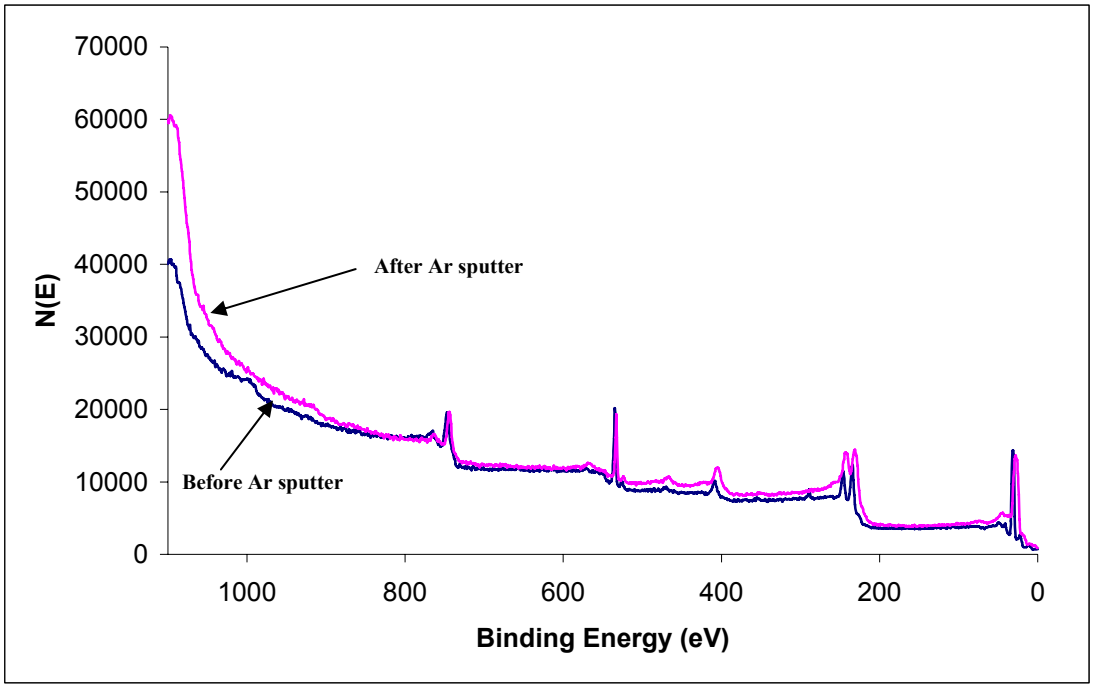

Figure 12: XPS scan of Ta_2O_5 film (calcined in O_2 at 1000°C)

	Binding energy	**Atomic concentration before Ar sputter**	**Atomic Concentration after Ar sputter**
O 1s	531 eV	63.7 %	60.4 %
C 1s	285 eV	13.8 %	0.9 %
Ta $4f_{5/2}$	24 eV	22.6 %	38.7 %

Figure 13: XPS table of assignment

X-ray diffraction analysis: Identification of the phases of the resulting oxide film was performed via XRD on a Rigaku DMAX® XRD system with Cu (Kα) radiation. (fig. 14)

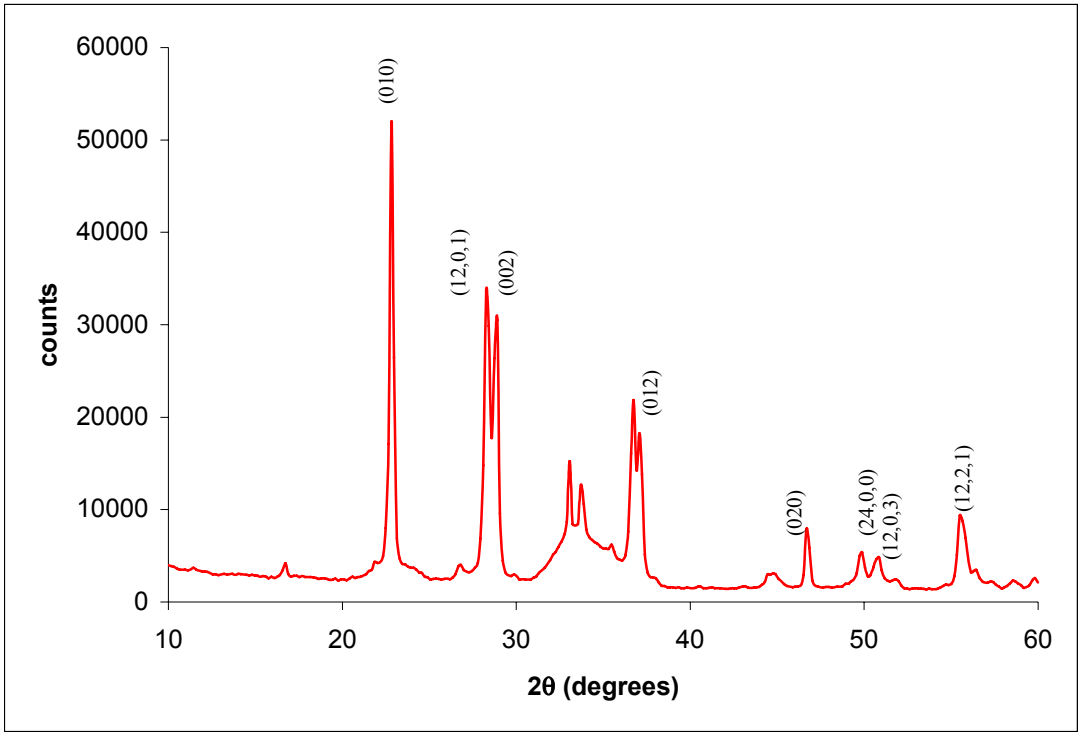

Figure 14: XRD spectrum of Ta_2O_5 film (calcined in O_2 at 1000°C)

TGA analysis: Thermogravimetric analysis was performed to elucidate the change in physical properties that occurs through the calcination cycle to yield the final oxide film. Analysis was performed on a TGA7/DSC7 Perkin Elmer® system. Samples were heated from ambient temperature to 1000ºC at a rate of 1.6ºC/min under a steady O_2 flow of 20cm^3/min and finally held at 1000ºC for 10 hours. (fig. 15)

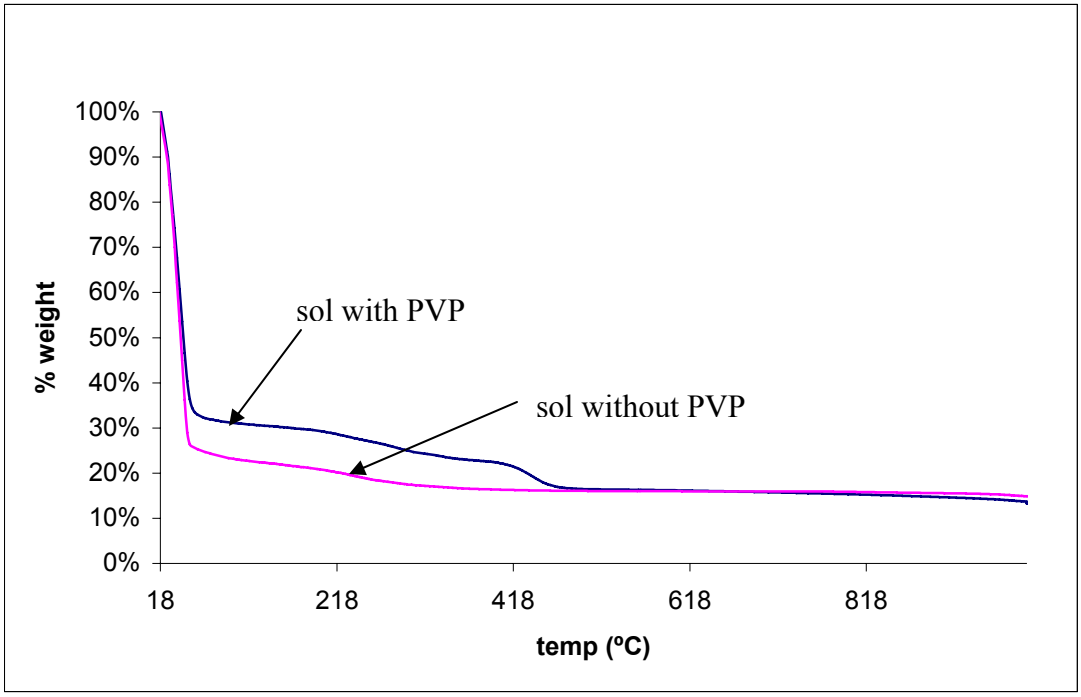

Figure 15: TGA analysis of Ta_2O_5 sol precursor with PVP and without PVP

Discussion

The ^1H spectrum is of a characteristic 2-methoxyethoxide type of coordination[30, 31] (fig. 7 & 8). The triplet at 3.7 ppm on the ^1H spectrum corresponds to a CH_2 hydrogen of a carbon bound to another CH_2 whose hydrogen signal appears at about 3.48ppm (triplet) and is bound to an O atom.[30] The singlet at 3.38ppm corresponds to CH_3 hydrogen bound to an oxygen atom. The ^{13}C spectrum confirms the above coordination with the methyl carbon at 58.8ppm, the oxygen bonded CH_2 carbon at 73.6ppm and the adjacent CH_2 carbon at 61.7 ppm (fig. 9).[30] The broad region in the ^1H appearing around 2.7 ppm is also observed in a sample of the original $Ta(OCH_2CH_3)_5$ in the same NMR standard as used above. NMR spectra of samples with $CaSO_4$ pellet yielded identical spectra to the ones above, thus showing that the broad band is not due to water present in the sample. The source of this band is still under investigation.

The NMR spectra suggest that the ethoxide ligands around the Ta metal center are exchanged for the $-OCH_2CH_2OCH_3$ ligand. There is no trace of any ethoxide/ethanol, hence we can conclude that the exchanged ethoxide liganda are removed as ethanol during the vacuum evaporation stage of synthesis. The coordination of the Ta cannot be

deciphered from this analysis, but the suggested product is $Ta(OCH_2CH_2OCH_3)_5$ via the reaction:[4, 9, 32-34]

$$Ta(OCH_2CH_3)_{5(l)} + 5HOCH_2CH_2OCH_{3(l)} \rightarrow Ta(OCH_2CH_2OCH_3)_{5(l)} + 5HOCH_2CH_{3(l)}$$

Alternatively, the NMR signature could be purely from the solvent and the Ta metal center could be immobilized via Ta-O bonds to the PVP molecule.[21] Proton NMR spectrum of 2-methoxyethanol yields a quartet centered at 3.7 ppm. The occurrence of a triplet for this sample suggests the existence of deprotonated OH group possibly due to extensive hydrogen bonding. Presence of the Ta-O and Ta-O-C bonds is verified by the FTIR bands < 1000 cm^{-1}. Band assignments are listed in fig. 4.

Analysis of sols at different points in time via both NMR and FTIR does not show any change in chemical composition of the sol (fig. 5 & 6). This suggests that the difference observed in film thickness and microstructure from sols of different age is either a physical effect, namely the binder interaction with the $Ta(OCH_2CH_2OCH_3)_{5(l)}$ (or the Ta metal center) and solvent, or a modification of the binder molecular chain arrangement. PVP is capable of hydrogen bonding via the C=O functional group, though findings in this work suggest that there could be more than H-bonding taking place. Given the large size of the PVP molecule chains, it is most likely that the freshly synthesized sols have highly crosslinked PVP molecules. The sol precursor exhibits bands at 1603 and 1540 cm^{-1} that are absent from the control and comparison spectra. These bands fall in the regions where non cyclic amino and amido modes are expected (hydroxyamic C=O (1600-1800 cm^{-1}) and C-N stretching (1525-1575 cm^{-1}) bands, amide N-H in plane bending (1515-1570 cm^{-1}) and primary alkylamic NH_2 scissoring (1610-1650))[26]. This suggests that there could be an alteration of the polymeric structure that is undetectable by NMR experiments. This is supported by the microstructure observed in the green films resulting from fresh sols (fig. 11). The polycondensed oxide particles are about 822 nm in diameter (fig. 11(a)). As time goes by, there is by further polycondensation of the oxide network giving larger particle sizes in the films derived from sols subjected to greater ageing (933 nm) (fig. 11(b)). SEM micrographs of green films from aged sols show particle sizes of about 1.11μm diameter (fig. 11(c)).

General polycondensation sequence of reaction is as follows:[4, 33, 34]

Hydrolysis: $2\ M(OR)_4 + 2\ H_2O \rightarrow 2\ (RO)_3M\text{-}OH + 2\ ROH$

Subsequent condensation reactions involving the hydroxyl groups yield networks composed of inorganic oxide (M-O-M) linkages.

Olation: $2\ (RO)_3M\text{-}OH \rightarrow (RO)_3M\text{-}O\text{-}M(OR)_3 + H_2O$

Oxolation: $(RO)_3M\text{-}OH + M(OR)_4 \rightarrow (RO)_3M\text{-}O\text{-}M\ (RO)_3 + ROH$

This is also supported by the thinner, denser films resulting from aged sols in comparison to fresh sols subjected to identical deposition spin rate, implying a less crosslinked matrix (fig. 10) due to growth of M—O—M particles.

Acetylacetone has been observed to not only slow down the rate of hydrolysis and polycondensation but also to significantly influence the morphology and crystallinity of the final product of the sol gel synthesis.[35, 36] In this synthesis, acetylacetone is seen as likely to cause crosslinking of PVP molecules. The spherical polycondensed oxide particles are not present in control sols (without acetylacetone) until the sol ages and turns turbid as seen in the SEM images (fig. 11 (d)-(f)). This is further evidence as to the open network that allows for greater penetration of moisture in the crosslinked sol upon exposure to ambient conditions, resulting in greater hydrolysis. Given that the green films without acetylacetone are denser than the ones with acetylacetone, and that the FTIR data taken over time does not show any changes in the relative hydrogen bonding peaks it is less probable that the extensive pore structure in the latter is due to pure hydrogen bonding.

TGA results show an initial drop in mass up to 50ºC attributed to solvent evaporation (fig. 15). Between 60ºC and 500ºC there is a change in the rate of decrease in % weight, with the PVP assisted sample showing a slower rate of change than the sample without PVP. There is a significant increase in the rate of decrease of % weight at 450 ºC, which is attributable to a change in structure from amorphous to orthorhombic Ta_2O_5. Beyond 500ºC the rate of change in % weight is relatively similar for both samples. This supports the hypothesis that the presence of PVP serves to relieve tensile stress within the film upon thermal treatment up to about 500ºC when all the binder is pyrolised.[22, 28] The slower rate of decrease in % weight signifies slower change in the film microstructure, a plasticity that allows differential expansion between the film particles and substrate with minimal or no cracking of the film.

XPS data reveals 13.8% carbon content that is reduced to 0.9% upon sputtering with argon, confirming ambient contamination as the carbon source. This shows that the removal of PVP is complete and there is negligible residual carbon. The Ta:O ratio confirms atomic coordination as Ta_2O_5 (fig. 12 & 13).

XRD pattern identifies the film obtained as orthorhombic Ta_2O_5. The spectrum matches ICSD card # 97-004-7493 with Miller indices labeled in fig. 14.

Conclusion

PVP has been shown as an effective binder material in the sol gel synthesis of thick Ta_2O_5 films for high temperature applications. This study was undertaken to investigate the effect of PVP binder in the sol precursor via NMR, FTIR, TGA, XPS, SEM, and XRD analytical tools. It has been reported that the type of Ta_2O_5 films obtained from sols of different ages varies in thickness and microstructure, suggesting that there was a progressive change occurring in the composition of the sol precursor with time. It was found that incorporation of PVP in the presence of acetylacetone results in extensive crosslinking of the sol matrix. This serves to relieve tensile stresses generated in the film during solvent removal and thermal treatment due to thermal mismatch between the deposited film and the substrate. The resulting films are found to be stable and crack free. With time, there is continued polycondensation of the Ta—O—Ta network yielding denser, thinner films with particles of larger diameter.

Acknowledgments: SEM, XRD and XPS analysis was carried out in the Center for Microanalysis of Materials, University of Illinois, which is partially supported by the U.S. Department of Energy under grant DEFG02-91-ER45439

References:

Ganley, J. C.; Seebauer, E. G.; Masel, R. I., Porous anodic alumina microreactors for production of hydrogen from ammonia. *Aiche Journal* **2004,** 50, (4), 829-834.
Ganley, J. C.; Thomas, F. S.; Seebauer, E. G.; Masel, R. I., A priori catalytic activity correlations: the difficult case of hydrogen production from ammonia. *Catalysis Letters* **2004,** 96, (3-4), 117-122.

Fleming, J. G.; Lin, S. Y.; El-Kady, I.; Biswas, R.; Ho, K. M., All-metallic three-dimensional photonic crystals with a large infrared bandgap. *Nature* **2002,** 417, (6884), 52-55.
Hass, D. D. P., D.; Glass, D. E.; Wiedemann, K. E *Reflective Coating on Fibrous Insulation for Reduced Heat Transfer*; August, 1997; p^pp.
Viskanta, R., Overview of convection and radiation in high temperature gas flows. *International Journal of Engineering Science* **1998,** 36, (12-14), 1677-1699.
Mir, J. M.; Agostinelli, J. A., Optical Thin-Films for Wave-Guide Applications. *Journal of Vacuum Science & Technology a-Vacuum Surfaces and Films* **1994,** 12, (4), 1439-1445.
Ozer, N.; Lampert, C. M., Structural and optical properties of sol-gel deposited proton conducting Ta2O5 films. *Journal of Sol-Gel Science and Technology* **1997,** 8, (1-3), 703-709.
Ezhilvalavan, S.; Tseng, T. Y., Preparation and properties of tantalum pentoxide (Ta2O5) thin films for ultra large scale integrated circuits (ULSIs) application - A review. *Journal of Materials Science-Materials in Electronics* **1999,** 10, (1), 9-31.
Chaneliere, C.; Autran, J. L.; Devine, R. A. B.; Balland, B., Tantalum pentoxide (Ta2O5) thin films for advanced dielectric applications. *Materials Science & Engineering R-Reports* **1998,** 22, (6), 269-322.
Beinhorn, F.; Ihlemann, J.; Simon, P.; Marowsky, G.; Maisenholder, B.; Edlinger, J.; Neuschafer, D.; Anselmetti, D., Sub-micron grating formation in Ta2O5-waveguides by femtosecond UV-laser ablation. *Applied Surface Science* **1999,** 139, 107-110.
Kukli, K.; Aarik, J.; Aidla, A.; Kohan, O.; Uustare, T.; Sammelselg, V., Properties of Tantalum Oxide Thin-Films Grown by Atomic Layer Deposition. *Thin Solid Films* **1995,** 260, (2), 135-142.
Corbella, C. V., M.; Pinyol, A.; Porqueras, C.; Person, C.; Bertran, E., Influence of the porosity of RF sputtered Ta2 O5 thin films on
their optical properties for electrochromic applications. *Solid State Ionics* **2003,** 165, 15-22.
Toki, K.; Kusakabe, K.; Odani, T.; Kobuna, S.; Shimizu, Y., Deposition of SiO2 and Ta2O5 films by electron-beam-excited plasma ion plating. *Thin Solid Films* **1996,** 282, (1-2), 401-403.
Werder, D. J.; Kola, R. R., Microstructure of Ta2O5 films grown by the anodization of TaNx. *Thin Solid Films* **1998,** 323, (1-2), 6-9.
Joshi, P. C.; Cole, M. W., Influence of postdeposition annealing on the enhanced structural and electrical properties of amorphous and crystalline Ta2O5 thin films for dynamic random access memory applications. *Journal of Applied Physics* **1999,** 86, (2), 871-880.
Liu, L.; Wang, Y.; Gong, H., Annealing effects of tantalum films on Si and SiO2/Si substrates in various vacuums. *Journal of Applied Physics* **2001,** 90, (1), 416-420.
Kozuka, H.; Takenaka, S.; Tokita, H.; Okubayashi, M., PVP-assisted sol-gel deposition of single layer ferroelectric thin films over submicron or micron in thickness. *Journal of the European Ceramic Society* **2004,** 24, (6), 1585-1588.
Kozuka, H.; Kajimura, M.; Hirano, T.; Katayama, K., Crack-free, thick ceramic coating films via non-repetitive dip-coating using polyvinylpyrrolidone as stress-relaxing agent. *Journal of Sol-Gel Science and Technology* **2000,** 19, (1-3), 205-209.

Chen, W.; Zhang, J. Y.; Fang, Q.; Li, S.; Wu, J. X.; Li, F. Q.; Jiang, K., Sol-gel preparation of thick titania coatings aided by organic binder materials. *Sensors and Actuators B-Chemical* **2004,** 100, (1-2), 195-199.
Chen, Y. Y.; Wei, W. C. J., Formation of mullite thin film via a sol-gel process with polyvinylpyrrolidone additive. *Journal of the European Ceramic Society* **2001,** 21, (14), 2535-2540.
Jia, Q. X.; Mccleskey, T. M.; Burrell, A. K.; Lin, Y.; Collis, G. E.; Wang, H.; Li, A. D. Q.; Foltyn, S. R., Polymer-assisted deposition of metal-oxide films. *Nature Materials* **2004,** 3, (8), 529-532.
Kishimoto, T.; Kozuka, H., Sol-gel preparation of TiO2 ceramic coating films from aqueous solutions of titanium sulfate (IV) containing polyvinylpyrrolidone. *Journal of Materials Research* **2003,** 18, (2), 466-474.
Subramanian, V. N., N.; Seebauer, E. G.; Shannon, M. A.; Masel, R. I., Synthesis of PVP assisted Ta2O5 Films and its Characterization. *Thin Solid Films* **2005,** in press.
Fidalgo, A.; Ilharco, L. M., Thickness, morphology and structure of sol-gel hybrid films: I - The role of the precursor solution's ageing. *Journal of Sol-Gel Science and Technology* **2003,** 26, (1-3), 363-367.
Smith, B., *Infrared Spectral Interpretation: A systematic Approach*. ed.; CRC Press: Boca Raton, Florida (USA), 1999; 'Vol.' p.
Coates, J., Interpretation of Infrared Spectra, A Practical Approach. In *Encyclopedia of Analytical Chemistry*, ed.; Meyers, R. A., 'Ed.'^'Eds.' John Wiley & Sons, Ltd: Chichester, 2000; 'Vol.' p^pp 10815-10837.
Phule, P. P., Sol-Gel Synthesis of Ferroelectric Lithium Tantalate Ceramics - Ftir Investigation of the Molecular Modification of Tantalum Ethoxide. *Journal of Materials Research* **1993,** 8, (2), 334-338.
Kozuka, H.; Higuchi, A., Single-layer submicron-thick BaTiO3 coatings from poly(vinylpyrrolidone)-containing sols: Gel-to-ceramic film conversion, densification, and dielectric properties. *Journal of Materials Research* **2001,** 16, (11), 3116-3123.
Kelly, P. V.; Mooney, M. B.; Beechinor, J. T.; O'Sullivan, B. J.; Hurley, P. K.; Crean, G. M.; Zhang, J. Y.; Boyd, I. W.; Paillous, M.; Jimenez, C.; Senateur, J. P., Ultraviolet assisted injection liquid source chemical vapour deposition (UVILS-CVD) of tantalum pentoxide. *Advanced Materials for Optics and Electronics* **2000,** 10, (3-5), 115-122.
Kim, Y.; Chae, H. K.; Lee, K. S.; Lee, W. I., Preparation of SiBi2Ta2O9 thin films with a single alkoxide sol-gel precursor. *Journal of Materials Chemistry* **1998,** 8, (11), 2317-2319.
Werndrup, P.; Verdenelli, M.; Chassagneux, F.; Parola, S.; Kessler, V. G., Powders and dense thin films of late transition metal oxide nanocomposites from structurally characterized single-source precursors. *Journal of Materials Chemistry* **2004,** 14, (3), 344-350.
Clem, P. G.; Jeon, N. L.; Nuzzo, R. G.; Payne, D. A., Monolayer-mediated deposition of tantalum(V) oxide thin film structures from solution precursors. *Journal of the American Ceramic Society* **1997,** 80, (11), 2821-2827.
Brinker, C. J.; Scherer, G. W., Sol-gel science-the physics and chemistry of sol-gel processing. *Academic press, inc.1250 sixth avenue,San Diego,CA,92101* **1990**.
Hubert-Pfalzgraf, L. G., Toward molecular design of homo and heterometallic precursors of lanthanide oxide-based materials. *New J. Chem* **1995,** 19, 727- 750.

Nakagawa, K.; Wang, F. M.; Murata, Y.; Adachi, M., Effect of acetylacetone on morphology and crystalline structure of nanostructured TiO2 in titanium alkoxide aqueous solution system. *Chemistry Letters* **2005,** 34, (5), 736-737.
Maslosh, V. Z.; Kotova, V. V.; Maslosh, O. V., Effect of acetylacetone on the residual content of formaldehyde in urea-formaldehyde resin. *Russian Journal of Applied Chemistry* **2002,** 75, (8), 1369-1370.